RSC Advances

PAPER

View Article Online
View Journal | View Issue

Cite this: *RSC Adv.*, 2014, **4**, 7483

Folic acid modified superparamagnetic iron oxide nanocomposites for targeted hepatic carcinoma MR imaging†

Zhongling Wang,[ab] Jing Zhu,[c] Yinyin Chen,[a] Kaiming Geng,[c] Nong Qian,[b] Liang Cheng,[d] Ziwei Lu,[a] Yue Pan,[c] Liang Guo,*[a] Yonggang Li*[a] and Hongwei Gu*[c]

Received 16th October 2013
Accepted 19th November 2013

DOI: 10.1039/c3ra45878d

www.rsc.org/advances

A novel targeted MRI contrast agent for tumor cells and tumor over-expressing affinity receptor was synthesized and characterized. Dopamine (DA) was used to present functional molecules on the surface of superparamagnetic iron oxide nanoparticles (SPIONs), and dextran was conjugated with the folic acid (FA) that forms stable nanocomposites. The T_2 values of the targeted and non-targeted nanoparticles at 3.0 T were 10.9 ms and 11.8 ms, respectively. The T_2 relaxivity values (r_2) were 91.7 s^{-1} mM^{-1} and 84.7 s^{-1} mM^{-1}, respectively. The results of the competitive inhibition test suggest that the SPION-DA-dextran-FA uptake is associated with folate receptor binding. In the *in vitro* study, the T_2 signal intensity of hepatic carcinoma cells (Bel 7402) incubated with the folate targeting nanocomposites decreased significantly. In contrast, the T_2 signal did not show an obvious decrease for cells treated with the non-targeting nanocomposites. In the *in vivo* study, the T_2 signal decreased significantly 18 hours after injection of the folate targeting contrast agent. In contrast, the maximum intensity of the non-targeting group appeared 0.5–2 hours after injection and the T_2 signal intensities recovered gradually 4 hours after injection. Our results indicated that FA targeting SPIONs have the ability for use as a novel targeting MRI contrast agent and have a better targeting tropism to the Bel 7402 cells and tumor.

1. Introduction

In recent years, magnetic resonance imaging (MRI) has become one of the most useful diagnostic techniques in providing noninvasive and real time detection of diseases such as tumors *etc.*[1–3] Various contrast agents have been applied to improve the quality of MRI. Among these contrast agents, superparamagnetic iron oxide nanoparticles (SPIONs) have been intensively studied as promising MRI probes because of their nontoxicity, biocompatibility, large surface area and uniform physical properties such as good magnetic properties.[4–8] However, traditional SPIONs lack targeting abilities and also would be rapidly eliminated from the blood stream after injection which is due to their recognition by macrophages of the mononuclear phagocyte system (MPS).

SPIONs can be coated with lipids to improve their biocompatibility and enhance their circulation half-life in the blood stream. Several approaches have been reported, using materials such as dextran, poly(ethylene glycol) (PEG) or polyvinylpyrrolidone as coatings materials.[9–14] One way to increase the concentration of SPIONs to targeted tumors is to conjugate these nanoparticles with targeting molecules that have a high affinity to target tumors. One promising candidate is folic acid since its receptor is overexpressed on a variety of tumors of diverse origins.[15–22]

In this article, we report a general strategy that uses dopamine as the anchor to link folic acid on the surface of the SPIONs for hepatic carcinoma MR imaging.[23,24] Dextran is also introduced to improve the hydrophilicity and biocompatibility and also to prolong the circulation half-life of the folic acid modified SPIONs (Fig. 1). The resulting nanocomposites, that is, the SPIONs conjugated with dopamine, dextran and folic acid (SPION-DA-dextran-FA) were characterized by transmission electron microscopy (TEM), Fourier transform infrared spectroscopy (FTIR) and X-ray powder diffraction (XRD). *In vitro* experiments were performed using Bel 7402 cells, a human hepatic carcinoma cell line which over-expresses surface receptors for folic acid. And *in vivo* MR imaging was also performed. The aim of this study was to study the targeting function of FA-conjugated SPION-DA-dextran to hepatoma cells *via*

[a]*Department of Radiology, The First Affiliated Hospital of Soochow University, Soochow University, Suzhou, Jiangsu, 215006, China. E-mail: liyonggang224@163.com; ilguoliang@sohu.com*

[b]*Department of Imaging, The Second People's Hospital of Changzhou, Nanjing Medical University, Changzhou, Jiangsu, 213003, China*

[c]*Key Laboratory of Organic Synthesis of Jiangsu Province, College of Chemical, Chemical Engineering and Materials Science, Soochow University, Suzhou, Jiangsu, 215123, China. E-mail: hongwei@suda.edu.cn; Fax: +86-65880905; Tel: +86-65880905*

[d]*Functional Nano & Soft Materials Laboratory (FUNSOM), Soochow University, Jiangsu, Suzhou 215123, China*

† Electronic supplementary information (ESI) available. See DOI: 10.1039/c3ra45878d

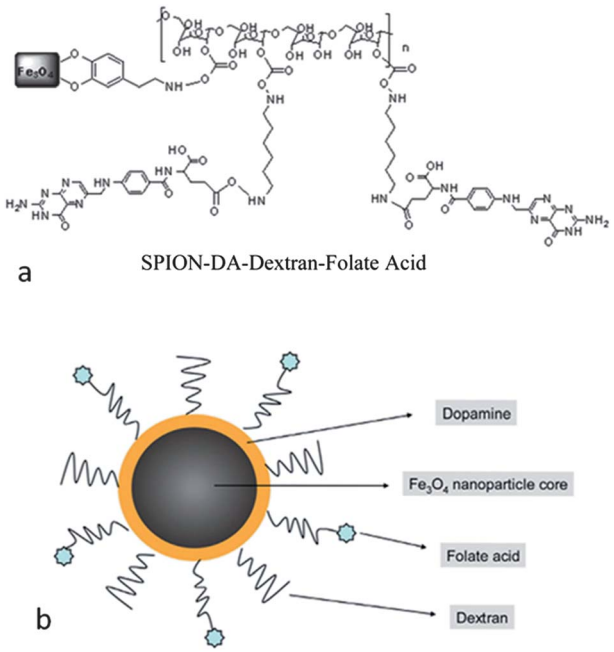

Fig. 1 (a) The chemical structure and (b) schematic representation of SPION-DA-dextran-folate acid (FA).

the FA receptor and to asses the feasibility for surveillance of tumor targeting with MRI.

2. Materials and methods

2.1 Synthesis of iron oxide nanoparticles

Iron oxide nanoparticles were synthesized using a reported procedure:[23,25] $FeCl_3 \cdot 6H_2O$ (2.7 g, 10 mmol) and sodium oleate (9.125 g, 30 mmol) were added to a mixture of ethanol (20 mL), deionized water (15 mL) and hexane (35 mL). The mixture was refluxed at 70 °C for 4 h; the upper reddish brown hexane solution containing the iron–oleate complex was then separated, and washed three times with deionized water (10 mL) in a separatory funnel. The hexane was then evaporated in a rotary evaporator to yield a dark reddish brown, oily iron–oleate complex. Using a standard Schlenk line, the iron oleate complex (9 g, 10 mmol) was dissolved in 25 g of 1-octadecene; oleic acid (1.41 g, 5 mmol) or sodium oleate (1.52 g, 5 mmol) was then added. The mixture was heated to 320 °C at a ramp of 3–5 °C min^{-1} for 30 min under argon. The resulting black nanocrystal solution was cooled to room temperature, and 2-propanol (50 mL) was added to precipitate the magnetic nanoparticles. After centrifugation, the nanoparticles were washed with hexane and ethanol three times, and then redispersed in hexane or toluene.

Dopamine hydrochloride (200 mg) was dissolved in dimethyl sulfoxide (DMSO) (20 mL), and then Fe_3O_4 (100 mg) in 10 mL DMSO was added. The mixture was stirred overnight at room temperature. The modified Fe_3O_4 nanoparticles were precipitated by adding ethanol, and collected by centrifugation at 6000 rpm. After washed with ethanol and hexane (5/1, v/v) three times, the product was re-dispersed in ethanol.

Activated dextran was synthesized following a literature method.[26] Firstly, a dextran solution was prepared in DMSO (30 mM). Next, five amounts of disuccinimidyl carbonate (DSC) dissolved in DMSO were added to the dextran solution with stirring. Five amounts of 4-dimethylamino pyridine (DMAP) in DMSO were then slowly added, and the solution was stirred for 6 h. Dextran was precipitated by a slow addition of acetone, and washed with acetone and DMSO using the precipitation–redispersion protocol. The activated dextran powder was dried and stored at 4 °C.

The method for conjugating the Fe_3O_4 nanoparticles to activated dextran was as follows: activated dextran (0.5 g) was dissolved in 30 mL of DMSO and then the DA-functionalized Fe_3O_4 nanoparticles dissolved in 10 mL DMSO were added slowly to the stirring solution of the above mixture. The mixture was stirred for 24 h at room temperature under nitrogen and then five amounts of 1,6-hexanediamine were added. After that, the mixture was washed with ethanol three times, and the product was re-dispersed in ethanol.

The *N*-hydroxysuccinimide ester of folic acid (NHS-folate) was prepared by a known procedure.[27]Folic acid (1 g, 2.26 mmol) was dissolved in 20 mL of dry dimethylformamide (DMF) to which 0.31 g (1.52 mmol) of dicyclohexylcarbodiimide (DCC) and 0.257 g (2.26 mmol) of NHS were added. The reaction mixture was stirred for 12 h at room temperature in the dark. The byproduct, dicyclohexylurea, was filtered off, and 100 mL of 30% acetone in diethyl ether was added with stirring. A yellow precipitate formed and was collected on a sintered glass crucible; after washing with acetone and ether several times, the material was used immediately for the next step in the synthesis.

The method for conjugating the Fe_3O_4 nanoparticles to folate was as follows: NHS-folate (0.5 g) was dissolved in 50 mL of dry pyridine and then the Fe_3O_4 nanoparticles were added slowly to the stirring solution of the above mixture. The mixture was stirred for 24 h at 25 °C under nitrogen, the mixture was reacting in dark, and collected by centrifugation at 6000 rpm. After washed with ethanol and hexane (1/5, v/v) three times, the product was re-dispersed in ethanol. The SPION-DA-dextran-FA was obtained.

2.2 Characterization

The average core size, size distribution and morphology were examined using a FEI TecnaiG20 transmission electron microscope (TEM) at a voltage of 200 KV. Fourier transform infrared spectroscopy (FTIR) measurements were recorded on a ProStar LC240 Fourier Transform Spectrophotometer. The UV-Vis spectroscopy of the nanoparticles was taken on a Beckman Coutler DU-800 UV-Vis spectrometer (Beckman Coutler, Fullerton, CA) with a 10 mm optical path length quartz cuvette. The hysteresis loop was measured with a Quantum Design SQUID MPMS XL-7 magnetometer at an applied field (H) of 9 kOe at 298 K.

The average core size and structural properties of IONP were characterized by X-ray powder diffraction (XRD) using a D/Max-III C X-ray diffractometer with monochromatized Au Ka radiation.

The T_2 values of the SPION-DA-dextran-FA and IONP-DA-dextran nanoparticles were measured at 3.0 T MRI Scanner

(GE Signa HDx, USA.) at room temperature. The T_2 relaxation times were measured using the following parameters: MR imaging was performed with a 3.0 T MR. T_2-weighted images were acquired using the following parameters: TR/TE, 1000 ms/108 ms; slice thickness, 1 mm; slice spacing, 1 mm; matrix, 256 × 256; FOV, 8 cm × 8 cm. The relaxivities r_2 (s^{-1} mM^{-1}) were obtained from the fitting of the $1/T_2$ *versus* plots.

2.3 Cell culture and animal model

Bel 7402, a human hepatic carcinoma cell line which stably express surface receptors for folic acid, was obtained from the Shanghai Academy of Life Sciences. Bel 7402 cells were cultured at 37 °C in folate-free DMEM 1640 medium (Gibco Co., Ltd USA) supplemented with 50 μg mL^{-1} penicillin, 50 μg mL^{-1} streptomycin and 10% fetal bovine and maintained in a humidified contained 5% CO_2 atmosphere.

Nude mice (20 g) were purchased from the Shanghai Laboratory Animal Center and the animal experiments were performed in accordance with the institute guide lines. 12 nude mice were injected with Bel 7402 cells *via* 0.2 mL (4×10^7 cells) folate-free DMEM 1640 medium suspension under the left armpit. All animals were maintained on a folate-free diet for 5 weeks, the mice were housed in polycarbonate microisolator cages and the tumor sizes were monitored per week. Tumors reaching a diameter of 1.0–1.2 cm after 8 weeks were used for in vivo MR imaging.

2.4 Prussian blue staining

Bel 7402 cells at a density of 1×10^6 cells per dish were washed, trypsinized after incubation for 1 h with SPION-DA-dextran-FA and SPION-DA-dextran at Fe concentrations of 40 μg mL^{-1} in a folate-free DMEM 1640 medium at 37 °C. Then cells were washed with phosphate-buffered saline (PBS) three times and fixed with 4% glutaraldehyde for 20 min, and incubated at 37 °C with 2 mL Prussian blue solution comprising equal volumes of a 2% hydrochloric acid aqueous solution and 2% potassium ferrocyanide(II) trihydrate for 30 min. After staining with 0.5% neutral red for 3 min, the iron staining was finally observed using microscope.

For histopathological analysis, liver samples were quickly obtained and fixed in a 10% neutral buffered formaldehyde solution, embedded in paraffin and sectioned. The 5 μm thick sections were stained with hematoxylin and eosin (HE), Masson's trichrome for collagen fiber and Prussian blue for iron.

2.5 Competitive inhibition experiment

Under experimental Fe concentrations (40 μg mL^{-1}), cells that were pre-treated with large amounts of free folic acid of different concentrations (0.5, 1.0, 1.5, 2.0 mmol L^{-1}) for 1 h before the targeting nanocomposite was added to the medium. MR imaging was performed with a 3.0 T MR. T_2-weighted images were acquired using the following parameters: TR 4240 ms; TE108 ms; slice thickness, 1 mm; slice spacing, 1 mm; matrix, 256 × 256; FOV, 8 cm × 8 cm. The T_2 signal intensities were measured within the region of interest.

2.6 *In vitro* cell cytotoxicity analysis

The Bel 7402 cell line was used to perform an MTT (methyl thiazolyl tetrazolium) test to determine the *in vitro* cell cytotoxicity of SPION-DA-dextran-FA and SPION-DA-dextran. An amount of 5×10^4 Bel 7402 cells were seeded on a 96 well plate in folate-free DMEM 1640 medium and then incubated for 24 h at 37 °C under 5% CO_2. After incubating the Bel 7402 cells for 18 h with the media containing SPION-DA-dextran-FA or SPION-DA-dextran at Fe concentration of 40 μg mL^{-1}, the supernatant was removed and the cells were washed three times with PBS. Absorption values were measured and recorded every day. For the MTT assay, 20 μL MTT stock solution (5 mg mL^{-1}) was added to each well, After incubating for 4 h, the medium was then removed and each well was treated with 150 μL dimethyl sulfoxide (DMSO) with pipetting, for 10 min. Cell viability was assessed by absorbance which was measured at 490 nm using a microplate reader.

2.7 *In vitro* MR imaging

Bel 7402 cells (1×10^6) were washed three times with PBS and incubated with SPION-DA-dextran-FA and SPION-DA-dextran, in a folate-free DMEM 1640 medium for 2 h, respectively, at Fe concentrations of 0, 5, 10, 20, 40 and 80 μg mL^{-1}. After digestion with 0.25% trypsin, the mixture was centrifuged at 1200 rpm for 4 min and resuspended in 0.5 mL of 1% agarose in an Eppendorf tube. MR imaging was performed with a 3.0 T MR. T_2-weighted images were acquired using the following parameters: TR 4240 ms; TE108 ms; slice thickness, 1 mm; slice spacing, 1 mm; matrix, 256 × 256; FOV, 8 cm × 8 cm. The T_2 signal intensities were measured within the region of interest.

2.8 *In vivo* MR imaging

Mice were anesthetized with 0.04 mL of 3% sodium pentobarbital by intraperitoneal injection. Tumor-bearing nude mice were divided into the experimental group ($n = 6$) and control group ($n = 6$) randomly. They were injected with an SPION-DA-dextran-FA solution and SPION-DA-dextran (0.2 mL) *via* tail vein respectively. The MR imaging of mice was performed using a 3.0 T MR imager and a high resolution animal coil. All samples were measured by a T_2-weighted spin-echo sequence (TR/TE = 4000/108 ms; slice thickness, 2 mm; slice spacing, 1 mm; matrix, 256 × 256; FOV, 8 cm × 8 cm). Tumor and muscle signal variation was observed after the injection of contrast agent at 0.5, 1, 2, 4, 8, 12, 18, and 24 hours and CNR was calculated at different time points.

2.9 Statistical analysis

All data are expressed as mean ± standard deviation (SD). Statistical analyses of the MRI signal intensity were performed with univariate Analysis of Variance, and a binary comparison between the mean were performed with the Student–Newman–Keuls (SNK) and LSD test. The analyses were performed using SPSS 17.0 software. We considered a difference to be statistically significant if the p value was less than 0.05.

3. Results and discussion

3.1 Preparation and characterization of nanoparticles

Nanoparticles were usually coated with a layer of biocompatible polymer such as polyethylene glycol (PEG), dextran, or dendrimers for surface modification. In the present research, we used a series of dextran molecules (MW = 40 000) coupled with dopamine. We followed the procedure published previously.[28] After ligand exchange, the nanocomposites were easily dispersed in water forming a clear solution. Then we used a targeting ligand, folate to functionalize the nanocomposites. These nanocomposites are stable in water and no aggregates were observed for several days.

The FTIR spectra of unmodified SPION and SPION-DA, SPION-DA-dextran and SPION-DA-dextran-FA are shown in Fig. 2. The IR spectra of Fig. 2d exhibits peaks at about the 1600–1610 cm^{-1} and 1680–1690 cm^{-1} ranges, which are characteristic of the FTIR spectra of folic acid.[5,29] In addition, the C–OH stretch vibrations of the dextran in the 1180–1200 cm^{-1} range are present in Fig. 2d. These results indicated that the folic acid had been coated successfully on the surface of the magnetic nanoparticles in the presence of dextran.

The UV-Vis spectra of SPION, SPION-DA-dextran, FA, SPION-DA-dextran-FA are shown in Fig. 3. The folic acid content (line c) can be obtained from the absorbance of 286 nm, which can be attributed to folic acid only. Since there is no absorption peaks at 286 nm for SPION (line a) and SPION-DA-dextran (line b), the absorbance of SPION-DA-dextran-FA at 286 nm confirms that the SPIONs are surface-modified with folic acid.

Fig. 4 shows the X-ray powder diffraction (XRD) patterns of SPION-DA-dextran-FA. From the XRD data, a series of characteristic peaks of Fe_3O_4 still exist after modification with DA-dextran-FA, compared with the JCPDS standard card. The XRD data shows that the crystalline Fe_3O_4 nanoparticles were not changed after surface modification.

To determine the magnetic properties of SPION-DA-dextran-FA, a SQUID magnetometer was used. The SPION-DA-dextran-FA were found to be superparamagnetic with a magnetization (M) value of 60 emu g^{-1} at an applied field (H) of 9 kOe at 298 K (Fig. 5). The hysteresis loop demonstrated that the coercivity and remanence are almost negligible, which is typically a superparamagnetic behaviour.

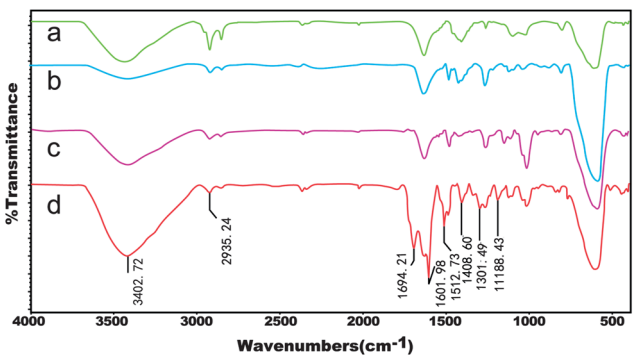

Fig. 2 The FTIR spectra of (a) SPION (Fe_3O_4); (b) SPION-DA; (c) SPION-DA-dextran; (d) SPION-DA-dextran-FA.

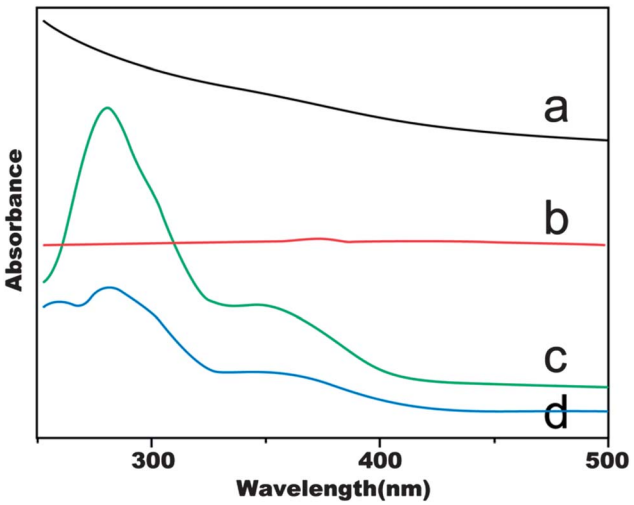

Fig. 3 The UV-vis spectra of (a) SPION (Fe_3O_4); (b) SPION-DA-dextran; (c) FA; (d) SPION-DA-dextran-FA.

Fig. 6 shows the TEM image of the as-prepared SPIONs. It can be found that the SPIONs are uniform with a diameter of about 14 nm. The dynamic light scattering (DLS) measurements showed that diameter was around 96 nm and 89 nm for SPION-DA-dextran-FA and SPION-DA-dextran, respectively (Table S1†). The T_2 values of the SPION-DA-dextran-FA and SPION-DA-dextran nanoparticles at 3.0 T were 10.9 ms and 11.8 ms, respectively. Their T_2 relaxivity values (r_2) were 91.7 mM^{-1} s^{-1} and 84.7 mM^{-1} s^{-1}, respectively (Table S1†).

3.2 Cytotoxicity study of SPION-DA-dextran-FA and SPION-DA-dextran

An MTT test assay using the (FR+) Bel 7402 cell line was carried out to analyze the potential cytotoxicity of SPION-DA-dextran and SPION-DA-dextran-FA. Cell viability was measured for 3 days. Fig. 7 shows that these modified SPION do not inhibit the

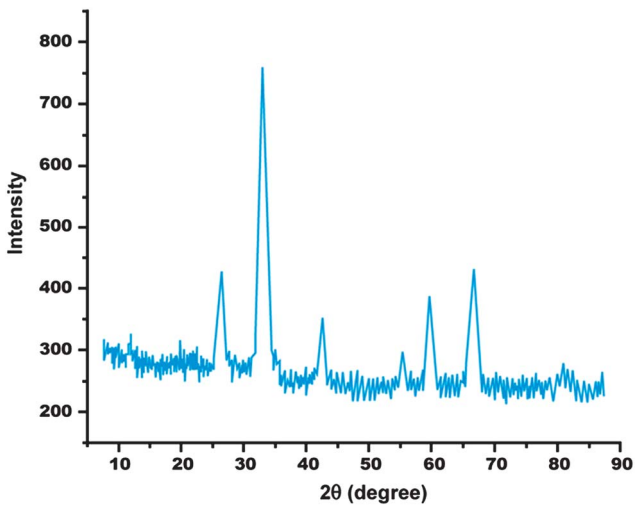

Fig. 4 The X-ray powder diffraction (XRD) pattern of SPION-DA-dextran-FA.

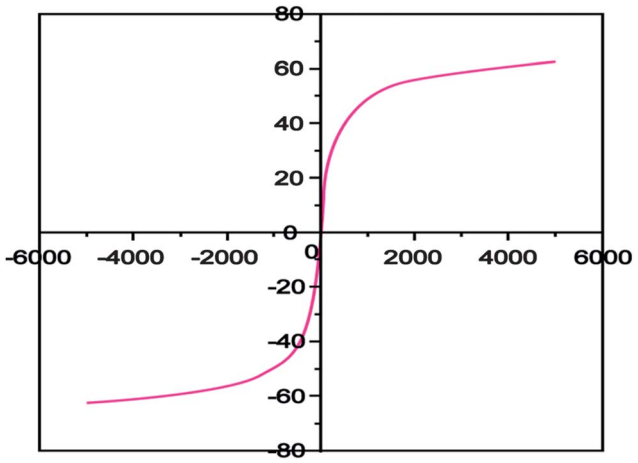

Fig. 5 The SPION-DA-dextran-FA were found to be superparamagnetic with a magnetization (M) value of 60 emu g^{-1} at an applied field (H) of 9 kOe at 298 K. Magnetic hysteresis loops of SPION-DA-dextran-FA measured at 298 K.

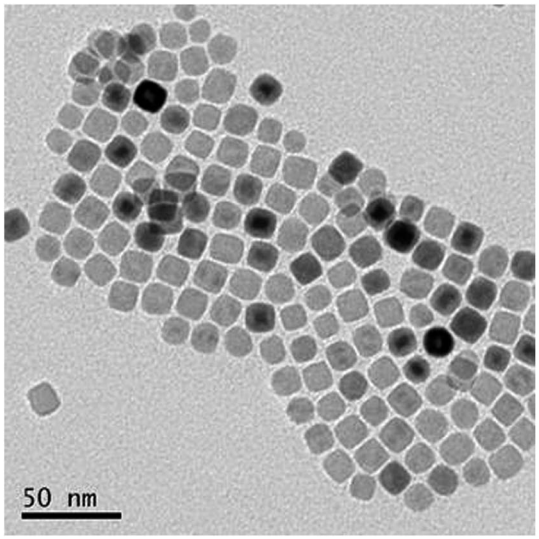

Fig. 6 The TEM image of as-prepared SPION.

Bel 7402 cell growth with up to 40 μg mL^{-1} of Fe. These results demonstrate that both SPION-DA-dextran and SPION-DA-dextran-FA are biocompatible and express low cytotoxicity.

3.3 Prussian blue staining

The presence of intracellular SPIONs in hepatoma cells was shown by Prussian blue staining. As shown in Fig. 8, Prussian blue staining experiments of *in vitro* and *in vivo* study evidenced that the cell uptake level of the nanocomposites strongly depended on the targeting ligand. For *in vitro* study, the cell experiments showed a much stronger blue appearance in the cells of the folate targeting nanocomposites group than the control group when the Fe concentration reached 40 μg mL^{-1} (Fig. 8a and b). For *in vivo* study, the blue areas in the experiment group could be seen in the tumor mass after 24 h injection

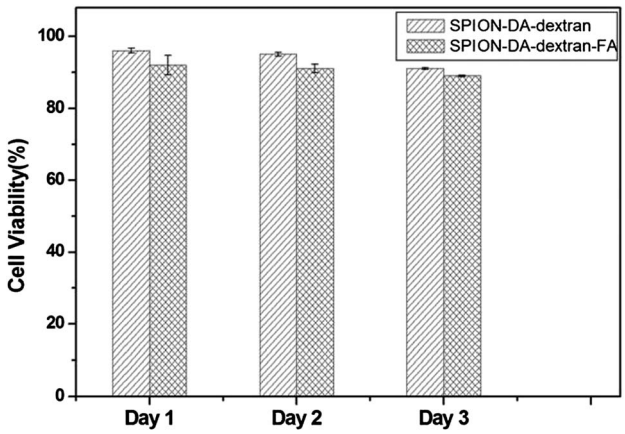

Fig. 7 The MTT test of Bel 7402 cells treated with SPION-DA-dextran and SPION-DA-dextran-FA (Fe concentration: 40 μg mL^{-1}).

of targeting contrast agents, while no obvious blue areas can be observed inside the tumor tissues of the control group (Fig. 8c and d). Obviously, the folate targeted nanocomposites have a good targeting ability for Bel 7402 cells and hepatic carcinoma. The Prussian blue staining of cells further evidenced the selective labeling of the FR-positive cells by SPION-DA-dextran-FA. Our results demonstrated the effective *in vitro* targeting of a specific type of cancer cells using SPION-DA-dextran-FA.

3.4 Competitive inhibition test

Fig. 9 demonstrates the change of the T_2 signal intensities when different concentrations of free folic acid were added to the culture medium before adding the targeting nanocomposites (Table S2†). Because of the blocking effect of FA, an increase in

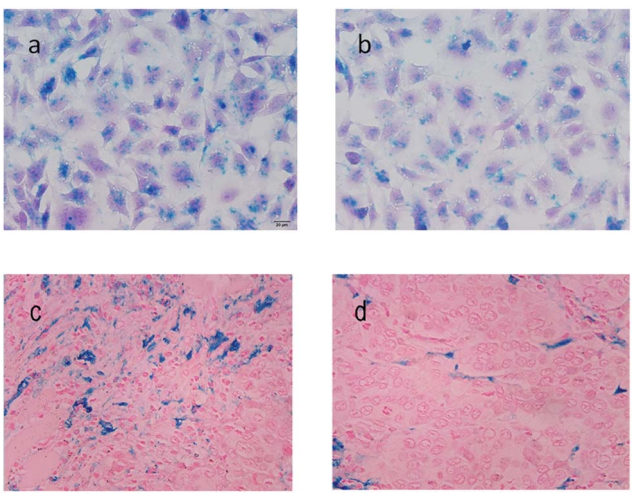

Fig. 8 Prussian blue staining (×200) of Bel 7402 cells (1×10^6) after 1 h incubation with folate targeted nanocomposites (a) and non-folate targeted nanocomposites (b) at an Fe concentration of 40 μg mL^{-1} in a folate-free DMMC 1640 medium. Colocalization of iron staining is detected in the tumor tissues after 24 h injection of targeting contrast agents (c). Blue areas are not seen in the tumor after 24 h injection of non-targeting contrast agents (d).

the signal intensity, resulting from a lower dose of SPION, was seen when the free folic acid concentration in the culture medium was higher. This result suggests that the uptake of SPION-DA-dextran-FA is associated with the folate receptor binding.

3.5 *In vitro* MRI studies

Prior to showing the specificity of the folate targeting nanocomposites for *in vivo* MRI, the signal intensity of cells on T_2-weighted decreased significantly with the exaltation of iron concentration in the SPION-DA-dextran-FA. The rate of the signal intensity variety was −89.76% at an iron concentration of 80 μg mL^{-1} in culture medium. No significant reduction of the signal intensity was found in SPION-DA-dextran and the rate of signal intensity variety was −37.92% (Fig. 10). The rate of the signal intensity variety for folate targeting nanoparticles by the Bel 7402 cells was about 2–3 times higher than that for the nontargeting nanoparticles. The T_2 signal intensity of the receptor-positive Bel 7402 cells incubated with SPION-DA-dextran-FA was significantly different compared with SPION-DA-dextran ($P < 0.01$) (Table S3†).

In recent years, one of the focuses of research in medical diagnostics is molecular imaging that can facilitate early diagnosis, providing fundamental information on pathological processes. The cellular imaging is developing rapidly in this field.[30] SIONPs have been intensively studied for these applications in biomedical science such as MRI contrast agents for cancer diagnosis and target-drug delivery.[31] In this study, the results from Fig. 10(a) and (b) indicate that the SPIONs play an important role in receptor-mediated endocytosis into the hepatic carcinoma cells. The tumor cells targeting events could be monitored with 3.0 T MR imaging.

3.6 *In vivo* MRI studies

To understand the tumor (FR+) and muscle uptake of folate targeting nanoparticles and nontargeting nanoparticles, MR imaging of tumor and muscle were observed at different time points after the injection of SPION-DA-dextran-FA (Fig. 11a) and

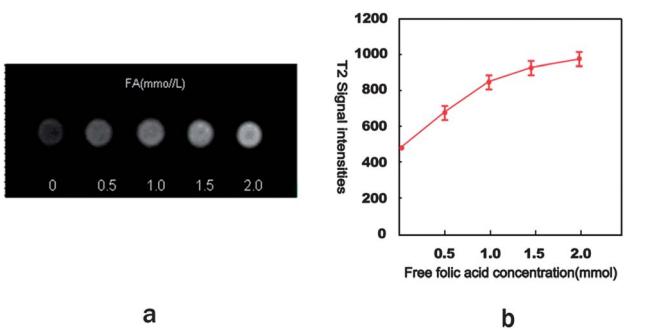

Fig. 9 T_2-weighted images of Bel 7402 cells (1×10^6) after a 1 h incubation with different concentration of free folic acid (0, 0.5, 1.0, 1.5, 2.0 mmol L^{-1}), followed by treatment with folate targeting nanocomposites for 1 h at an iron concentration of 40 μg mL^{-1} (a). Change of T_2 signal intensities with different concentrations of free folic acid were used (b).

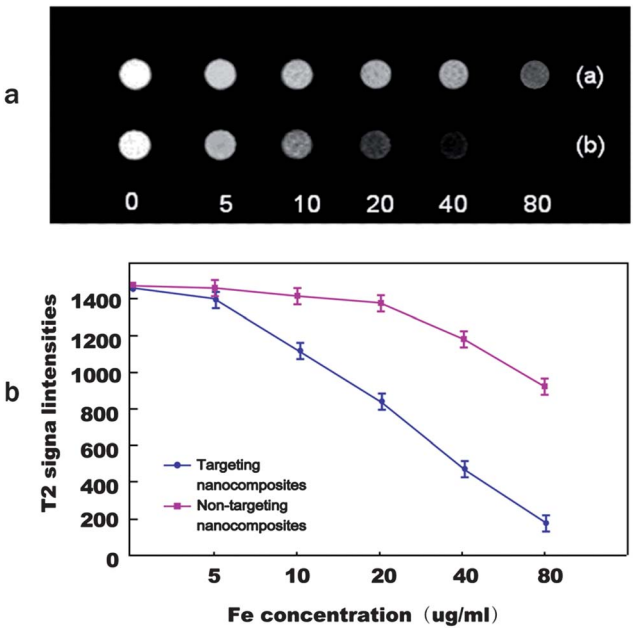

Fig. 10 (a) T_2-weighted images of Bel 7402 cells (1×10^6) after a 2 h treatment with different iron concentrations (0–80 μg mL^{-1}) of SPION-DA-dextran-FA ((b)) and SPION-DA-dextran nanocomposites ((a)). (b) Low T_2 signal intensities correlate with a high iron concentration (Targeting nanocomposites), reduction significantly of T_2 signal intensities when the iron concentration in culture media was higher (non-targeting nanocomposites), change of T_2 signal intensities was not obvious.

SPION-DA-dextran (Fig. 11c). We tested the feasibility of targeting using an animal (mice) model ($n = 12$) bearing Bel 7402 tumors. At 0.5 h after the injection of the folate targeting contrast agent, the T_2 signal slightly decreased in the tumors of nude mice and the T_2 signal decreased significantly after 18 hours injection of the folate targeting contrast agent, this effect is persistent up to the 24 h end point (Fig. 11b and d). The selective accumulation of the folate receptor-targeting nanoparticles in this tumor model was further confirmed by Prussian blue staining of tissue sections (Fig. 8c). We believe that the persistent tumor enhancement at 18 h postinjection of the folate-targeting nanoparticles is due to the folate receptor-binding effect. In addition to prolonged circulation which is a prerequisite for tumor accumulation of liposomes,[32,33] dextran is the best basis for a formulation that confers a long half-life in circulation. However, it may also be due to a passive targeting of the nanoparticles into the tumor resulting from the leakage of the agent into the tumor interstitium *via* capillaries present in tumors. These results showed that the folate-targeting nanoparticles were able to accumulate in hepatocellular tumors expressing the FR. In contrast, the maximum intensify of the nontargeting group appeared in 0.5–2 hours after injection. The T_2 signal intensities in the tumor recovered gradually after 4 hours injection of nontargeting contrast agent (Fig. 11,Table S4†). We did not detect a SPION-induced T_2 signal intensity change in the mouse-bearing 24 hours after the injection of nontargeting nanoparticles. On the other hand, the T_2 signal intensities varied in the muscle 0.5 h after the injection of the

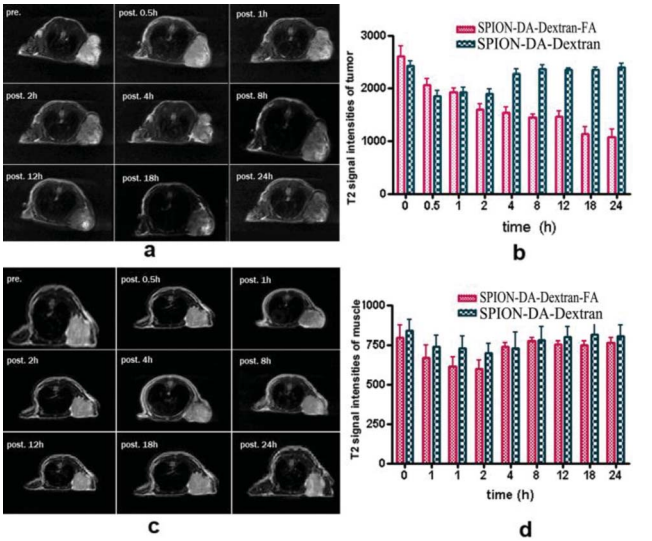

Fig. 11 The variation in the T_2 signal intensities of tumor and muscle after the injection of folate targeting contrast agent (a) and non-targeting contrast agent (c) 0.5 hour, 1 hour, 2 hour, 4 hour, 8 hour, 12 hour, 18 hour and 24 hour. The variation in the T_2 signal intensities of tumor (b) and muscle (d) at different time points.

folate targeting contrast agent and nontargeting contrast agent and the T_2 signal intensities recovered gradually 4 hours after the injection. The MR imaging variation in the muscle of the two groups were not statistically significant (Fig. 11 a, b and d, Table S4†). Here we have proven that SPION-DA-dextran-FA accumulates to a detectable amount in the tumor expressed with folate receptor.

4. Conclusion

We have successfully fabricated SPION modified by dextran conjugated with folic acid. By combining the biocompatibility and dispersivity of dextran with the specific cell targeting capability of FA, the SPION-DA-dextran-FA is hydrophilic, has an excellent dispersion and low cytotoxicity under the natural environment. Moreover, in this study, we proved that SPION-DA-dextran-FA has better targeting tropism to the human hepatic carcinoma cells and tumors *in vitro* and *in vivo* than SPION without modification by folic acid. SPION-DA-dextran-FA uptake is associated with folate receptor binding, and the cell targeting events could be monitored with the clinical MRI scanner as a noninvasive strategy. These folate targeted nanocomposites are believed to be efficient MR contrast agents.

Acknowledgements

This research is supported by the Jiangsu Province Natural Science Foundation of China (no. BK2006704-1). H.W.G. acknowledges the financial support of the National Natural Science Foundation of China (no. 21003092, 21373006), the Key Project of Chinese Ministry of Education (no. 211064), and the Priority Academic Program Development of Jiangsu Higher Education Institutions; Y.P. acknowledges financial support from the New Faculty Start Foundation of Soochow University (Q410900413); Y.G.L. acknowledges financial support from the National Natural Science Foundation of China (NSFC) (no. 81171394, 81171392), the Natural Science Fund of Jiangsu Province (no. BK2011307) and the Natural Science Fund for Colleges and Universities in Jiangsu Province (no. 09KJB320016).

Notes and references

1 L. Zhu, D. Wang, X. Wei, X. Zhu, J. Li, C. Tu, Y. Su, J. Wu, B. Zhu and D. Yan, *J. Controlled Release*, 2013, **169**, 228–238.
2 (*a*) C.-H. Fan, C.-Y. Ting, H.-J. Lin, C.-H. Wang, H.-L. Liu, T.-C. Yen and C.-K. Yeh, *Biomaterials*, 2013, **34**, 3706–3715; (*b*) J. Zhu, Y. Lu, Y. Li, J. Jiang, L. Cheng, Z. Liu, L. Guo, Y. Pan and H. Gu, *Nanoscale*, 2014, **6**, 199–202; (*c*) Y. Pan, M. J. C. Long, X. Li, J. Shi, L. Hedstrom and B. Xu, *Chem. Sci.*, 2011, **2**, 945–948; (*d*) J. Wu and C.-C. Chu, *J. Mater. Chem. B*, 2013, **1**, 353; (*e*) C. Xu and S. Sun, *Adv. Drug Delivery Rev.*, 2013, **65**, 732–743; (*f*) Y. G. Li, Y. J. Lu, H. Y. Hong, Y. Y. Chen, X. X. Ma, L. Guo, Z. L. Wang, J. H. Chen, M. Zhu, J. K. Ni, H. W. Gu, J. M. Lu and J. Y. Ying, *Chem. Commun.*, 2011, **47**, 6320–6322.
3 D. P. Cormode, T. Skajaa, Z. A. Fayad and W. J. M. Mulder, *Arterioscler., Thromb., Vasc. Biol.*, 2009, **29**, 992–1000.
4 W. B. Hyslop and R. C. Semelka, *Magn. Reson. Imaging*, 2005, **16**, 3–14.
5 T.-J. Chen, T.-H. Cheng, Y.-C. Hung, K.-T. Lin, G.-C. Liu and Y.-M. Wang, *J. Biomed. Mater. Res., Part A*, 2008, **87A**, 165–175.
6 G. A. F. van Tilborg, W. J. M. Mulder, N. Deckers, G. Storm, C. P. M. Reutelingsperger, G. J. Strijkers and K. Nicolay, *Bioconjugate Chem.*, 2006, **17**, 741–749.
7 Z. Zhou, L. Wang, X. Chi, J. Bao, L. Yang, W. Zhao, Z. Chen, X. Wang, X. Chen and J. Gao, *ACS Nano*, 2013, **7**, 3287–3296.
8 Y. Pan, X. W. Du, F. Zhao and B. Xu, *Chem. Soc. Rev.*, 2012, **41**, 2912–2942.
9 R. Y. Hong, B. Feng, L. L. Chen, G. H. Liu, H. Z. Li, Y. Zheng and D. G. Wei, *Biochem. Eng. J.*, 2008, **42**, 290–300.
10 C. C. Berry, S. Wells, S. Charles and A. S. G. Curtis, *Biomaterials*, 2003, **24**, 4551–4557.
11 Y. Zhang, N. Kohler and M. Zhang, *Biomaterials*, 2002, **23**, 1553–1561.
12 C. Corot, P. Robert, J.-M. Idée and M. Port, *Adv. Drug Delivery Rev.*, 2006, **58**, 1471–1504.
13 J. Wu, D. Wu, M. A. Mutschler and C.-C. Chu, *Adv. Funct. Mater.*, 2012, **22**, 3815–3823.
14 Y. Pan, M. J. C. Long, H.-C. Lin, L. Hedstrom and B. Xu, *Chem. Sci.*, 2012, **3**, 3495–3499.
15 P. S. Low, W. A. Henne and D. D. Doorneweerd, *Acc. Chem. Res.*, 2007, **41**, 120–129.
16 P. S. Low and A. C. Antony, *Adv. Drug Delivery Rev.*, 2004, **56**, 1055–1058.
17 S. Miotti, M. Bagnoli, F. Ottone, A. Tomassetti, M. I. Colnaghi and S. Canevari, *J. Cell. Biochem.*, 1997, **65**, 479–491.
18 G. Toffoli, C. Cernigoi, A. Russo, A. Gallo, M. Bagnoli and M. Boiocchi, *Int. J. Cancer*, 1997, **74**, 193–198.

19 N. Kamaly, T. Kalber, M. Thanou, J. D. Bell and A. D. Miller, *Bioconjugate Chem.*, 2009, **20**, 648–655.
20 J. Wu, Q. Liu and R. J. Lee, *Int. J. Pharm.*, 2006, **316**, 148–153.
21 R. Meier, T. D. Henning, S. Boddington, S. Tavri, S. Arora, G. Piontek, M. Rudelius, C. Corot and H. E. Daldrup-Link, *Radiology*, 2010, **255**, 527–535.
22 E. Sega and P. Low, *Cancer Metastasis Rev.*, 2008, **27**, 655–664.
23 C. Xu, K. Xu, H. Gu, R. Zheng, H. Liu, X. Zhang, Z. Guo and B. Xu, *J. Am. Chem. Soc.*, 2004, **126**, 9938–9939.
24 H. Gu, R. Zheng, X. Zhang and B. Xu, *J. Am. Chem. Soc.*, 2004, **126**, 5664–5665.
25 J. Jiang, H. Gu, H. Shao, E. Devlin, G. C. Papaefthymiou and J. Y. Ying, *Adv. Mater.*, 2008, **20**, 4403–4407.
26 C. Earhart, N. R. Jana, N. Erathodiyil and J. Y. Ying, *Langmuir*, 2008, **24**, 6215–6219.
27 S. Dhar, Z. Liu, J. r. Thomale, H. Dai and S. J. Lippard, *J. Am. Chem. Soc.*, 2008, **130**, 11467–11476.
28 J. Xie, C. Xu, N. Kohler, Y. Hou and S. Sun, *Adv. Mater.*, 2007, **19**, 3163–3166.
29 N. Kohler, G. E. Fryxell and M. Zhang, *J. Am. Chem. Soc.*, 2004, **126**, 7206–7211.
30 X. Huang, P. K. Jain, I. H. El-Sayed and M. A. El-Sayed, *Nanomedicine*, 2007, **2**, 681–693.
31 W. J. M. Mulder, A. W. Griffioen, G. J. Strijkers, D. P. Cormode, K. Nicolay and Z. A. Fayad, *Nanomedicine*, 2007, **2**, 307–324.
32 A. A. Gabizon, *Clin. Cancer Res.*, 2001, **7**, 223–225.
33 A. Gabizon, H. Shmeeda, A. T. Horowitz and S. Zalipsky, *Adv. Drug Delivery Rev.*, 2004, **56**, 1177–1192.